EXPERIMENTAL CELL RESEARCH 315 (2009) 1100–1116

available at www.sciencedirect.com

ScienceDirect

www.elsevier.com/locate/yexcr

Research Article

Identification and characterization of INMAP, a novel interphase nucleus and mitotic apparatus protein that is involved in spindle formation and cell cycle progression

Enzhi Shen[a], *Yan Lei*[a,1], *Qian Liu*[a,1], *Yanbo Zheng*[c], *Chunqing Song*[a], *Jan Marc*[d], *Yongchao Wang*[a], *Le Sun*[e], *Qianjin Liang*[a,b,*]

[a]*Key Laboratory of Cell Proliferation and Regulation Biology of Ministry of Education, College of Life Sciences, Beijing Normal University, Beijing 100875, PR China*
[b]*College of Life Sciences, Beijing Normal University, Beijing Key Laboratory, Beijing 100875, PR China*
[c]*The Institute of Medical Biotechnology (IMB) of the Chinese Academy of Medical Sciences, Beijing 100050, PR China*
[d]*School of Biological Sciences, University of Sydney, Sydney 2006, Australia*
[e]*AbMax Biotechnology Co., Haidian, Beijing 100085, PR China*

ARTICLE INFORMATION

Article Chronology:
Received 28 June 2008
Revised version received
20 January 2009
Accepted 20 January 2009
Available online 3 February 2009

Keywords:
Cell cycle
Cell proliferation
Mitosis
Spindle formation
Spindle-related protein
INMAP
HeLa cells
Sense RNA

ABSTRACT

A novel protein that associates with interphase nucleus and mitotic apparatus (INMAP) was identified by screening HeLa cDNA expression library with an autoimmune serum followed by tandem mass spectrometry. Its complete cDNA sequence of 1.818 kb encodes 343 amino acids with predicted molecular mass of 38.2 kDa and numerous phosphorylation sites. The sequence is identical with nucleotides 1–1800 bp of an unnamed gene (GenBank accession no. 7022388) and highly homologous with the 3′-terminal sequence of *POLR3B*. A monoclonal antibody against INMAP reacted with similar proteins in *S. cerevisiae*, Mel and HeLa cells, suggesting that it is a conserved protein. Confocal microscopy using either GFP-INMAP fusion protein or labeling with the monoclonal antibody revealed that the protein localizes as distinct dots in the interphase nucleus, but during mitosis associates closely with the spindle. Double immunolabeling using specific antibodies showed that the INMAP co-localizes with α-tubulin, γ-tubulin, and NuMA. INMAP also co-immunoprecipitated with these proteins in their native state. Stable overexpression of INMAP in HeLa cell lines leads to defects in the spindle, mitotic arrest, formation of polycentrosomal and multinuclear cells, inhibition of growth, and apoptosis. We propose that INMAP is a novel protein that plays essential role in spindle formation and cell-cycle progression.

Introduction

The mitotic spindle, a complex structure based on a bipolar array of microtubules and interacting proteins, is responsible for accurate segregation of duplicated chromosomes into two daughter cells during the cell cycle in all animals. The process of spindle formation involves dramatic reorganization of microtubules during the transition from interphase to M phase, with the microtubule

* *Corresponding author.* Key Laboratory of Cell Proliferation and Regulation Biology, College of Life Sciences, Beijing Normal University, Beijing 100875, PR China. Fax: +86 10 58807720.
E-mail addresses: Liangqianjin0059@163.com, Lqj@bnu.edu.cn (Q. Liang).
[1] These authors contributed equally to this work.

0014-4827/$ – see front matter © 2009 Elsevier Inc. All rights reserved.
doi:10.1016/j.yexcr.2009.01.022

minus ends being strictly focused on two opposite centrosomes and the plus ends assembling orderly in the equatorial region. Assembly of the structure and functional integrity of the spindle requires the involvement of numerous proteins as well as their appropriate spatio-temporal modifications. These proteins include centrosome-related factors like γ-tubulin, ninein, Pin1 and Aurora A [1–5]; NuMA, TPX2, NuSAP, 4.1R, EB1 and ASAP [6–11]; the small kinase Aik1, Ran GTPase, Nek2A [12–15]; microtubule-based motor proteins, and other proteins. Structural aberrations in these proteins either preclude the formation of mitotic spindles or the spindles are dysfunctional.

The identification and characterization of spindle-associated proteins have benefited our understanding of the structure and function of the spindle. The centrosome, which harbors hundreds of proteins, plays an important role as a microtubule-organizing center (MTOC) [16] and is responsible for the composition and assembly of the spindle. Aurora-A is among the essential centrosome-associated protein, and its silencing causes the formation of monopolar spindles [17,18]. Many spindle-associated proteins have been identified that are also essential for spindle assembly, for example, NuMA and NuSAP. In interphase, NuMA is dispersed throughout the nucleus whereas NuSAP localizes together with nucleolin to the nucleolus. During mitosis, in contrast, NuMA re-localizes to the spindle poles whereas NuSAP associates with the central spindle fibers in close contact with the chromosomes [9,19]. The cell cycle-dependent localization of these proteins is likely to facilitate their appropriate role in the structural integrity of the spindle and its function. Aberrant expression of these proteins has been linked to formation of multipolar spindles and other anomalies. Thus, overexpressing NuMA resulted in the formation of multipolarity [20] whereas deleting NuSAP caused the appearance of abnormal spindle including multipolarity and monopolarity, and overexpression of NuSAP caused bundling of cytoplasmic microtubules [9,21]. Nevertheless, in order to fully understand the composition and assembly of the spindle, undoubtedly additional spindle-associated proteins need to be identified and characterized.

Identification of novel proteins has been advancing rapidly with the development of new techniques like RACE, GFP labeling, and tandem mass spectrometry (MS/MS), as well as the application of autoantisera from patients with autoimmune diseases [22–24]. For example, NuMA was identified using an autoantiserum [25]. Moreover, new and important non-target proteins have been detected during the screening of cDNA libraries using autoantisera, for example, the identification of ICF45 which is involved in cell-cycle regulation [26].

Using an autoantiserum F46 [27] to screen HeLa cells cDNA expression library followed by MS/MS sequencing [28–31], we have identified a novel protein with apparent molecular mass of ~40 kDa. We named this protein Interphase Nucleus and Mitotic apparatus Associated Protein (INMAP). The cDNA sequence matches an unnamed gene (GenBank accession no. 7022388), with homologues in *S. cerevisiae*, HeLa and murine erythroleukemia (Mel) cells. Confocal microscopy using GFP fusion protein or monoclonal antibodies against INMAP revealed that the protein localizes to the interphase nucleus but associates specifically with the spindle during mitosis. The cell cycle-dependent localization was consistent with double immunolabeling of INMAP using antibodies against NuMA, γ-tubulin, and α-tubulin, and all four proteins also co-immunoprecipitated in their native state as a complex. Overexpression of INMAP in HeLa cell lines caused defects in spindle structure together with mitotic arrest and the formation of polycentrosomal and multinucleate cells, inhibited growth and induced apoptosis. We propose that INMAP is a novel protein that plays essential role in spindle formation and cell-cycle progression.

Materials and methods

Cell culture, reagents, and antibodies

HeLa and Mel cells were cultured in Dulbecco's modified Eagle's medium (DMEM) and RPMI Medium 1640 (Invitrogen, USA) containing 10% (v/v) fetal calf serum (FCS) (Invitrogen, New Zealand) at 37 °C in the presence of 5% CO_2. *S. cerevisiae* was cultured in PDA medium (200 g potato, 20 g glucose and 100 ml ddH_2O) at 28 °C. Other reagents were high-efficiency transfection reagent Vigofect (Vigoruse, Beijing, China), geneticin G418 (Merck, USA), rhodamine-conjugated goat anti-rabbit IgG, FITC-conjugated goat anti-mouse, and goat anti-human IgG (Victor Laboratories, Peterborough, UK). Oligonucleotides were synthesized by Sangon (Shanghai Sangon Biotechnology, Shanghai, China). Autoantiserum F46 was from a patient suffering from progressive systemic sclerosis (Peking Union Medical Hospital, China).

Cloning and sequencing of INMAP cDNA

HeLa cell cDNA expression library λEXlox (Novagen, Germany) was screened with autoantiserum F46 to identify positive cDNA clones. Positive cDNA clones were inserted into pEXlox plasmid by automatic subcloning according to the manufacturer's instructions. The 5′ end of *INMAP* cDNA was cloned by using the 5′-RACE method and SMART RACE cDNA amplification kit (Clontech, Japan). Template cDNA for the 5′-RACE was derived from RT-PCR HeLa total RNA using the primers GSP1, 5′ AAACAGTCACGTTCCATTTCCC 3′ for first PCR amplification, and NGSP1, 5′ TATCTAGCACCATGT-GTTTCAGC 3′ for nested PCR. The PCR products were inserted into TA cloning vector pMD18-T (Takara, Japan) and sequenced. The 5′-RACE products contained 1–806 bp of full-length cDNA and 1–3225 bp cDNA. The cDNA sequences were analyzed by BLASTN using NCBI GenBank nonredundant, expressed sequence tag (EST), and genomic databases. The derived protein sequence of INMAP was compared with the NCBI/EMBL protein database using BLASTP.

Immunoprecipitation and sequencing of INMAP protein

Whole HeLa-cell extracts were incubated with autoantiserum F46 (1:100 dilution) at 4 °C overnight and then incubated with Protein A plus-sepharose (Dingguo Biotechnology, Beijing, China). The beads were washed three times with phosphate-buffered saline (PBS) containing 0.1% Triton X-100, and bound proteins were eluted by heating at 100 °C for 5 min. The eluted proteins were separated by SDS-PAGE using 12% gels. The polypeptide band of interest was excised and digested in-situ with trypsin, and the resulting peptides were submitted for protein sequencing by Tandem Mass Spectrometry (MS/MS). The protein sequence of INMAP was used to search for homologous proteins in the NCBI/EMBL protein database using BLASTP.

Monoclonal antibody production

The coding sequence of *INMAP* was amplified by PCR using the pMD18-T-*INMAP* plasmid as a template. The primers were 5′ TCAGGATCCGGCTTTGGGCGTTGC 3′ and 5′ TCAGGATCCACTTCTGCTTTCCGTTG 3′. The PCR product was then cleaved with BamHI and inserted into the corresponding restriction sites in pGEX-2Z (constructed by pGEX-2T at the multiple-cloning site). Recombinant protein was expressed in BL21 (DE3) cells induced with 0.5 mM isopropyl-1-thio-β-D-galactopyranoside (IPTG), and the purified protein was submitted for the preparation of monoclonal antibodies (Welson Biotechnology, Beijing, China).

Construction of recombinant pEGFP expression vectors with INMAP or INMAP fragments and transient transfection of HeLa cell

Expression vectors for GFP-INMAP fusion protein were constructed by PCR amplification of *INMAP* cDNAs using the primers sequences 5′ TTGAAGCTTGGCTTTGGGCGTTGC 3′ and 5′ TCAGGATCCACTTCTGCTTTCCGTTG 3′. The PCR products were then cleaved with HindIII/BamHI and inserted into corresponding restriction sites in pEGFP-C3 (gift from Dr. Wanjie Li, Beijing Normal University, China). Deletion fragments of INMAP sequence corresponding to amino acid residues 1–100 and 95–343, were constructed by PCR amplification of the INMAP cDNA using the following pairs of primer sequences: 5′ GGAATTCCAATGGGGCCCATGTTG 3′ and 5′ CGGGATCCACGCCTTGTCTGTCTCA 3′; 5′ GGAATTCCAATCAAAATGCTGCTG 3′ and 5′ CGGGATCCCGTCATTCATTGTACTT 3′. The PCR products were then cleaved with EcoRI/BamHI and inserted into corresponding restriction sites in pEGFP-C3. The recombinant vectors were transiently transfected into HeLa cells by using high-efficiency transfection reagent Vigofect according to the manufacturer's instructions (Vigoruse, Beijing, China). Forty eight hours after transfection, cells expressing GFPfusion protein were observed with Olympus laser-scanning confocal microscope (Olympus Fluoview FV300, Japan).

Construction of sense-INMAP expression recombinant vector

A pcDNA3.1 (+) sense-*INMAP* vector was constructed by PCR amplification of the entire coding sequence of *INMAP* using pMD18-T-*INMAP* as a template. The PCR product was ligated in positive orientation into EcoRI/HindIII sites of pcDNA3.1(+) vector (gift from M.S Zhitao Rong, Beijing Normal University, China), and the fidelity of ligation was confirmed by sequencing using the primers 5′ GGAATTCCGATACACCAATCAGAC 3′ and 5′ CCCAAGCTTCCTCATTCATTGT 3′.

Selection of cell lines stably overexpressing INMAP

Recombinant vector pcDNA3.1(+) sense-*INMAP* or empty vector pcDNA3.1(+) were transfected into HeLa cells by using high-efficiency transfection reagent Vigofect according to the manufacturer's instruction (Vigoruse, Beijing, China). Stably transfected cells were selected with geneticin G418 (60 ng/ml) for 14 days, and transgenic cell lines stably overexpressing INMAP were established. The cells were then either fixed with 3. 7% paraformaldehyde for immunostaining or processed for protein extraction and immunoblot analysis.

Cell growth curves

Stably transfected HeLa cells expressing pcDNA3.1(+) sense-*INMAP* or empty vector pcDNA3.1(+) were seeded in 96-well plates at a density of 1×10^4 cells per well in DMEM containing 10% FCS, and grown at 37 °C in the presence of 5% CO_2. Cells were harvested and processed with MTT reagent as before [27].

Cell synchronization

HeLa cells in exponential phase of growth were washed with PBS and prepared for flow cytometry as control group. For synchronization at the mitotic phase, those were obtained by two methods. One was that the cells were transferred into fresh DMEM containing 10% FCS and 200 ng/ml nocodazole (Sigma, USA), and cultured at 37 °C in 5% CO_2 for 16 h. The other was that cells in mitotic phase were released from the bottom of the plate by gently shaking the plates, and collected by centrifugation. The synchronized cells and control cells were analyzed by flow cytometry.

Flow cytometry

Cells were collected by centrifuging, washed four times with cold PBS, and then fixed with 70% ethanol at 4 °C overnight. Following digestion with RNase for 30 min at 37 °C, propidium iodide (PI) (Sigma, USA) was added to a final concentration of 65 μg/ml. Flow cytometric analysis was performed on a FACS Calibur (BD Biosciences, USA).

Co-immunoprecipitation of INMAP with α-tubulin, NuMA, and γ-tubulin

HeLa cells in the exponential phase were washed with PBS and lysed in HEPES buffer (50 mM HEPES, pH 7.5, 150 mM NaCl, 1 mM $MgCl_2$, 1 mM EGTA) containing protease inhibitors (Beijing Nucleiprotein Bio-tech Co., Ltd. Beijing, China) and 0.5% Triton X-100 for 5 min on ice. Protein extracts were clarified by centrifugation for 10 min at 16,000 *g* at 4 °C. For immunoprecipitation, the extracts were incubated with antibodies against INMAP, NuMA, γ-tubulin, or α-tubulin overnight at 4 °C, followed by adding Protein A plus-Sepharose and incubating for 4 h at 4 °C. After centrifuging for 30 s at 4 °C, the pellets were washed five times with 500 μl of cell-lysis buffer while keeping on ice. Washed pellets of protein complexes were resuspended in 20 μl SDS sample buffer, vortexed, boiled, centrifuged for 30 s, and analyzed by SDS-PAGE and Western blotting. To ensure the co-immumoprecipitations are specific, we also used a monoclonal antibody against Golgin-245 (kindly provided by Professor Marvin J. Fritzler, University of Calgary, Alberta, Canada).

Western blot analysis

Total protein extracts of HeLa, Mel, *S. cerevisiae* cells or *E. coli* cells expressing GST-INMAP fusion protein were loaded onto 12% gels, separated by SDS-PAGE, and transferred onto a nitrocellulose membrane for 3 h at 200 mA. The membrane with transferred polypeptides was immersed in 5% skim milk in PBST (PBS containing 0.1% Tween20) at room temperature for 30 min. After rinses with PBST three times for 5 min each, the membranes with separated polypeptides were probed with anti-α-tubulin or anti-

INMAP monoclonal antibody (1:500) at room temperature for 1 h. POLR3B was detected using an anti-POLR3B monoclonal antibody (Abnova, Walnut, CA, USA). The membranes were then incubated with alkaline phosphatase-conjugated horse anti-rabbit IgG or goat anti-mouse IgG (1:500), and the immunoreactions detected with nitro-blue tetrazolium/5-bromo-4-chloro-3-indolyl phosphate (NBT/BCIP) (Promega, USA).

Immunostaining of cells

HeLa cells that were grown on coverslips, or were adhering to coverslips by centrifugation, were washed with PHEM (25 mM HEPES, 10 mM EGTA, 60 mM PIPES, 2 mM $MgCl_2$, pH 6.9) and fixed with 3.7% paraformaldehyde at room temperature for 15 min. This was followed by permeabilization with 0.5% Triton X-100 at room temperature for 90 s. After washing once with PHEM and twice with PBS, followed by blocking with 5% skim milk in PBS for 30 min at 37 °C, the coverslips were incubated with primary antibodies for 1 h at 37 °C. The primary antibodies were as follows: a mouse anti-INMAP monoclonal antibody (1:50), mouse anti-γ-tubulin polyclonal antibody (1:100) (Santa Cruz Biotechnology, USA), and rabbit anti-α-tubulin polyclonal antibodies (1:300) (Proteintech Group, Inc, USA), rabbit anti-γ-tubulin monoclonal antibody (1:300) (Medical and Biological Laboratories Co., LTD, USA), rabbit anti-NuMA monoclonal antibody (1:300) (Medical and Biological Laboratories Co., LTD, USA), rabbit anti-Nucleolin polyclonal antibody (1:300) (Medical and Biological Laboratories Co., LTD, USA) and rabbit anti-Centrin 1 polyclonal antibody (1:100) (Abcam, USA). The cells were then washed three times for 5 min each in PBST, and incubated for 1 h at 37 °C with the secondary antibodies. The secondary antibodies used were FITC-conjugated goat anti-mouse IgG (1:100), rhodamine-conjugated goat anti-rabbit IgG (1:100) (Vector Laboratories, Peterborough, UK). The cells were then washed three times with PBST, counterstained with propidium iodide (PI) or diamidio-2-phenylindole (DAPI) (Sigma, USA), and mounted in antifade mounting solution. The preparations were observed with Olympus laser-scanning confocal microscope (Olympus Fluoview FV300, Japan).

Results

Identification of interphase nucleus- and mitotic apparatus-associated protein (INMAP)

Screening HeLa cell cDNA expression library λEXlox using autoantiserum F46 from an autoimmune patient [27] detected several positive clones. We inserted the cDNA clones into pEXlox vector by automatic subcloning, and followed by MS/MS sequencing. Sequence analysis with BLASTN using EST and GenBank nonredundant databases revealed that one of the positive clones corresponds to nucleotides 779–1800 bp of an unnamed, uncharacterized gene (GenBank accession no. 7022388) and also to the 3′-terminal sequence of polymerase (RNA) III (DNA directed) polypeptide B (*POLR3B*) [32]. The 779–1800 bp cDNA fragment also contains two copies of a consensus polyadenylation signal sequence ATAAA [33] and a 3′-terminal polyadenylation tail. To determine the full-length gene, we applied 5′-RACE to clone the missing 5′-terminal sequence including the transcription start codon. This method produced an 806 bp sequence and a 3225 bp sequence. Using Vector NTI 6.0 software, we aligned the sequences of the two products with the human genome database and obtained two genes. One is consistent with the *POLR3B* gene sequence, whereas the other is identical to the entire cDNA sequence of the unnamed gene above except for an additional polyadenylation tail at the 3′-terminus. We named the protein according to its properties (see below) as Interphase Nucleus and Spindle Associated Protein (INMAP).

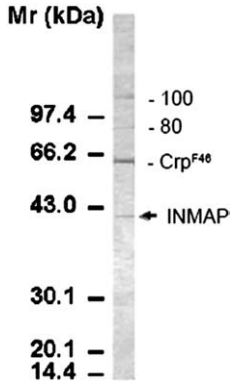

Fig. 1 – Western blot analysis of HeLa proteins using autoantiserum F46. Total HeLa cell proteins were separated by SDS-PAGE, transferred onto nitrocellulose membrane, and probed with F46 serum. The distinct ~60-kDa band corresponds to centrosome-related protein Crp^{F46} described previously [27]. The identities of the ~80 and ~100-kDa bands (bars) are unknown. The ~40-kDa polypeptide (arrow) was sequenced by Tandem Mass Spectrometry (MS/MS) and eventually identified as INMAP.

To confirm the identity of the *INMAP* gene, we used the autoantiserum F46 to immunoprecipitate the INMAP from total HeLa cell extract, followed by Western immunoblotting. The immunoblot revealed distinct polypeptide bands of Mr ~40, ~60, ~80 and ~100 kDa (Fig. 1). The ~60-kDa band has already been identified and characterized as centrosome-related protein Crp^{F46} [27]. The ~80 and ~100-kDa bands are far above the expected molecular mass of the predicted INMAP protein. The band of ~40 kDa is most likely the target protein INMAP according to its predicted molecular mass (see Fig. 2). Tandem mass spectrometry (MS/MS) of this polypeptide band (Table 1) showed that the amino-acid sequence is identical to the predicted amino-acid sequence of the unnamed gene (Fig. 2) including their translation initiation and termination sites.

The full-length *INMAP* cDNA is 1818 bp, which encodes a 343 amino-acid polypeptide with predicted molecular mass of 38.2 kDa (PeptideMass software) [34] and isoelectric point of 8.36. Analysis of the INMAP protein sequence using NetPhos 2.0 Server (http://www.cbs.dtu.dk/services/NetPhos/) [35,36] identified fourteen phosphorylation sites, including six Ser, four Thr and four Tyr, with main phosphorylation sites for PKC and cdc2.

Conservation of INMAP in eukaryotes

Sequence analysis of the predicted protein INMAP using BLASTP [37] and the NCBI database indicated that it is highly conserved in eukaryotes. To confirm the predicted conservation, we obtained an anti-INMAP monoclonal antibody by subcloning the entire coding sequence of *INMAP* into pGEX-2Z, inducing expression of the

Fig. 2 – Alignment of the nucleotide sequence of an unnamed gene (GenBank accession no. 7022388) with the human INMAP nucleotide sequence and its predicted amino acid sequence. Sequences of amino acid residues obtained by MS/MS are underlined. The start codon ATG and the stop codon TGA are boxed in black. Fourteen residues predicted to be phosphorylation sites are underlined with short bars. Amino acid residues SPGEK (boxed in grey) are highly similar to the phosphorylation site "S/T-P-X-K/R" for cell-cycle kinase P34^{cdc2}. Two copies of consensus polyadenylation signal sequence ATAAA are underlined in grey.

recombinant protein in BL21 cells, and submitting the purified protein for the preparation of a monoclonal antibody. Western blotting of total cell extracts from HeLa, murine erythroleukemia (Mel), and *S. cerevisiae* cells with the monoclonal antibody revealed the presence of immunoreactive polypeptides in all three species (Fig. 3A). The bacterially expressed GST-INMAP fusion protein appeared as a doublet in the Mr ~60–65-kDa region, indicating that the recombinant INMAP itself (without the ~25-kDa GST) is ~40 kDa. As expected, the HeLa protein extract again showed a distinct immunoreactive band at Mr ~40 kDa, which is close to predicted molecular mass of INMAP, as well as an additional band at about twice its size at ~80 kDa. In Mel cells, a single band appeared at Mr ~35 kDa, whereas the *S. cerevisiae* again showed two bands, one at Mr ~40 kDa and one at ~45 kDa. Thus the INMAP appears to be conserved in eukaryotes, albeit with variation in its molecular mass and a tendency to migrate on gels as two separate bands in a single species. This variation may be related to dimerization and also to the distinct structural and functional properties of these cell types.

Since the amino acid sequence of INMAP is homologous to the C-terminal domain of POLR3B, we compared the immunoblot of total proteins from HeLa cells, Mel cells, and *S. cerevisiae* obtained using the anti-INMAP antibody in Fig. 3A with a similar blot probed with an anti-POLR3B antibody (Fig. 3B). This showed immunoreactive bands at the expected POLR3B mass of ~130 kDa [32] but no reactions at lower molecular masses. Conversely, the anti-INMAP antibody did not react with any polypeptide in the 130-kDa

Table 1 – Results of protein sequencing by MS/MS

m/z submitted	MH^+ matched	Delta ppm	Start	End	Peptide sequence	Modifications
752.3673	752.3653	2.6647	316	321	(R) IPYACK(L)	
856.5237	856.5508	−31.5825	153	160	(K) LIELLAGK(A)	
951.4591	951.4688	−10.2044	189	196	(R) HGYNYLGK(D)	
1006.4705	1006.4515	18.8309	181	188	(K) DVCEDLVR(H)	
1033.5217	1033.4737	46.4292	307	315	(K) SSCHVSSLR(I)	
1478.7030	1478.6833	13.3174	168	180	(R) FHYGTAFGGSKVK(D)	1PO4
1537.7514	1537.7936	−27.4147	79	92	(K) VMISSNAEDAFLIK(M)	

region (Fig. 3A), indicating it recognizes specifically INMAP. Subcellular localizations obtained with the anti-INMAP antibody (see below) and with the anti-POLR3B antibody (details not shown) were also unrelated.

In order to examine the origin of the 80-kDa polypeptide in HeLa cells, we added 8 M urea to the protein sample followed by SDS-PAGE and testing for epitope reactivity with the anti-INMAP monoclonal antibody. The 8 M urea treatment apparently eliminated the 80-kDa immunoreactive band while increasing the intensity of the 40-kDa band, confirming that the 80-kDa polypeptide is indeed a dimer of 40 kDa (Fig. 3C).

Localization of INMAP to interphase nucleus, mitotic spindle, and midbody in HeLa cells

In order to explore the subcellular localization and dynamic distribution of INMAP in the cells, we constructed a recombinant expression vector *GFP-INMAP* and transfected it into HeLa cells. After transient transfection for 36 h, the GFP-INMAP fusion protein localized as distinct dots of various sizes and fluorescence intensities in the interphase nucleus (Fig. 4A). Remarkably, however, in mitotic cells the GFP-INMAP fusion proteins re-localized specifically to the mitotic spindle apparatus.

To exclude the possibility that the subcellular localization of INMAP may be influenced by the GFP tag, we performed indirect immunofluorescence microscopy using the monoclonal antibody against INMAP. The localization patterns obtained was similar to that with the GFP-INMAP fusion protein. Again, the INMAP localized as many dots of various sizes in the interphase nucleus and then re-localized to the mitotic spindle during prophase and metaphase (Fig. 4B). Although the signal intensity diminished somewhat during anaphase in some preparations, it again consistently localized as a strong signal with the midbody during telophase/cytokinesis.

To examine in more detail the localization of INMAP in relation to major spindle markers, we performed double immunostaining using antibodies against α-tubulin, NuMA, and γ-tubulin. The INMAP co-localized with α-tubulin, the main component of the mitotic spindle and the midbody, from prophase through to telophase and cytokinesis (Fig. 4C). INMAP also co-localized accurately with NuMA, which is known to associate with the spindle and the midbody, from prophase through to telophase and cytokinesis (Fig. 4D). However, in interphase nuclei the NuMA formed a matrix of numerous, fine puncta, unrelated to the relatively fewer and larger INMAP dots. Localization of INMAP in the interphase nucleus was unrelated to the distinct perinuclear signal of γ-tubulin, a classical marker of the centrosome, as expected (Fig. 4E). During mitosis, however, the extensive INMAP signal along the radiating arms of the spindle pole and the spindle pole itself was clearly superimposed over the sharply defined γ-

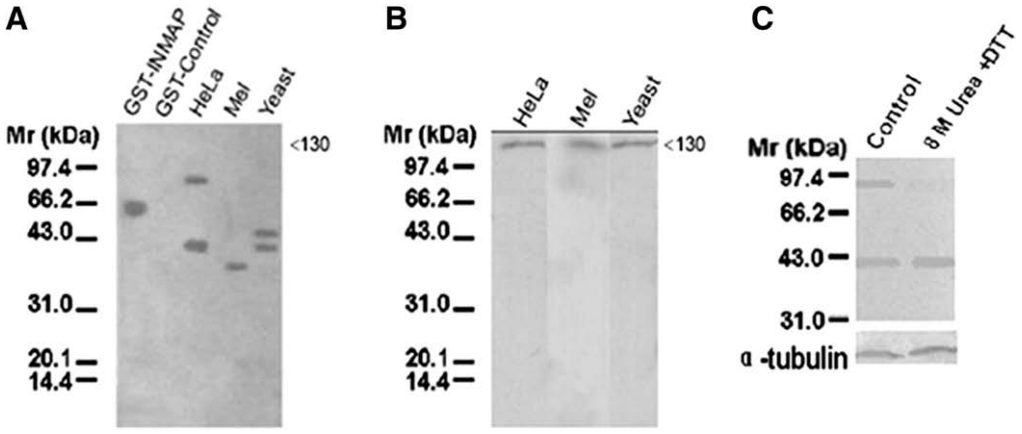

Fig. 3 – Western blot analysis of protein extracts of various species using anti-INMAP antibody. (A) Total proteins from *E. coli* expressing GST-INMAP or GST, or total proteins from HeLa cells, Mel cells, and *S. cerevisiae* were separated by SDS-PAGE, transferred onto nitrocellulose membrane, and probed with anti-INMAP monoclonal antibody. (B) Immunoblot of total proteins from HeLa cells, Mel cells, and *S. cerevisiae* were probed with anti-POLR3B antibody, showing immunoreactive bands at the expected position of ~130 kDa but absence of reactions at lower molecular masses as detected with the anti-INMAP antibody in (A). Conversely, the anti-INMAP antibody shows no immunoreactions at ~130 kDa. (C) A sample of total protein from HeLa cells was made with 8 M urea, the proteins separated by SDS-PAGE, and probed with anti-INMAP antibody. Disappearance of the ~80-kDa immunoreactive band and increased immunoreaction at ~40 kDa indicates that the ~80-kDa polypeptide is a dimer.

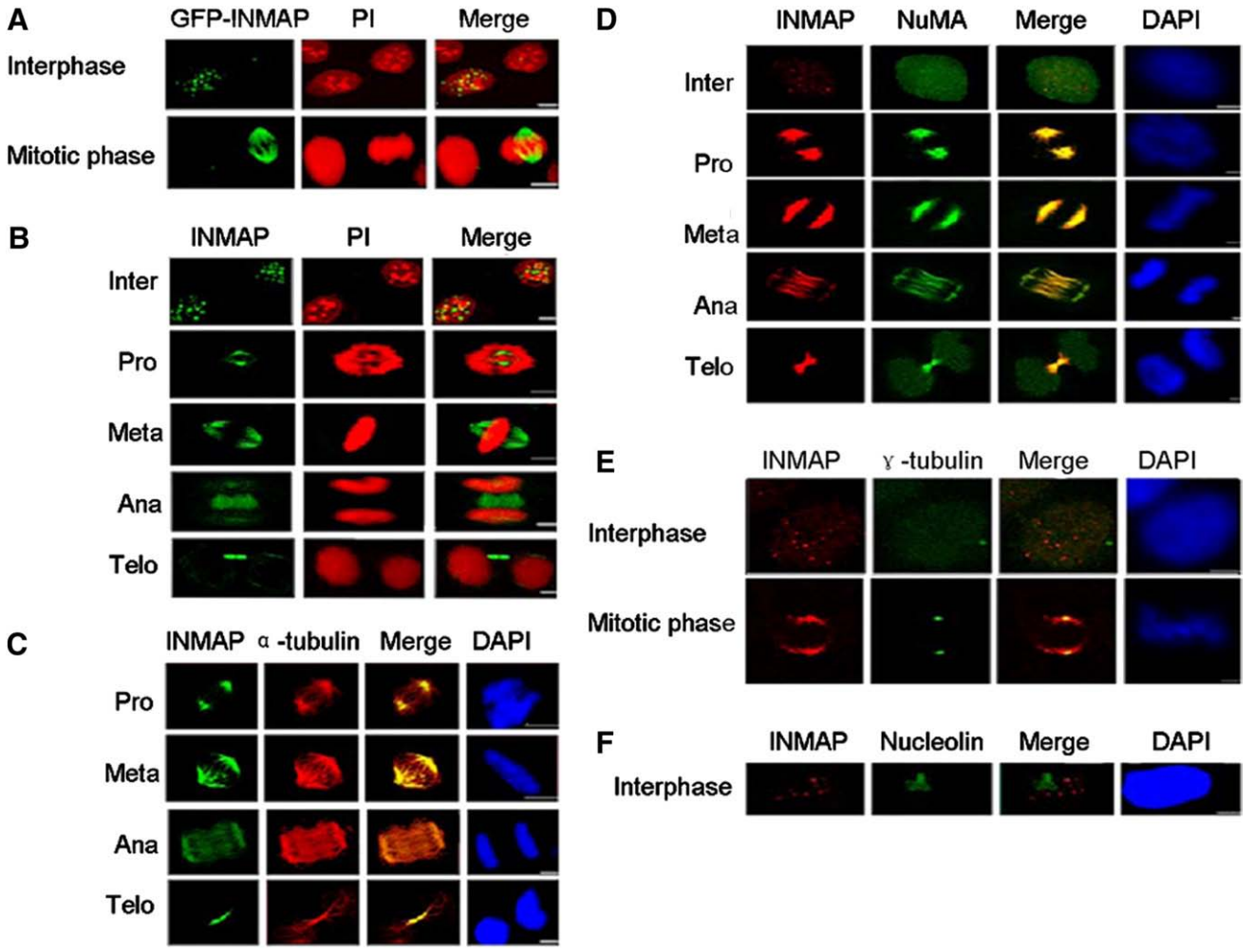

Fig. 4 – Localization of INMAP to interphase nucleus, mitotic spindle, and the cytokinetic midbody. HeLa cells expressing GFP-INMAP fusion protein (A) or labeled with antibodies (B–F) were counter-stained with propidium iodide (PI) or DAPI to label DNA, and examined by confocal microscopy. (A) GFP-INMAP fusion protein (green) appeared as discrete dots in the interphase nucleus (red), but at the onset of mitosis the signal re-localized specifically to the spindle. (B) Immunofluorescence localization using a monoclonal antibody against INMAP (green) again showed discrete dots in the interphase nucleus (red), followed by re-localization of the signal to the spindle during prophase, metaphase, anaphase, and to the midbody during telophase/cytokinesis. (C) Double immuno-labeling of INMAP (green) with an antibody against α-tubulin (red) as a spindle marker and merged images show that the two proteins co-localize (yellow) throughout mitosis and cytokinesis. (D) Double immuno-labeling of INMAP (red) with an antibody against NuMA (green) again showed co-localization (yellow) throughout mitosis and cytokinesis. However, in contrast to the discrete INMAP dots in the interphase nucleus (blue), the NuMA formed a matrix of numerous fine puncta throughout the cytoplasm as well as in the nucleus. (E) Double immuno-labeling of INMAP (red) with an antibody against γ-tubulin (green) as a centrosome marker. The distinct INMAP dots in the interphase nucleus (blue) are unrelated to the γ-tubulin in the centrosome in the perinuclear region; however, during mitosis the two proteins clearly co-localize (yellow) at the spindle pole. (F) Double immuno-labeling of INMAP (red) with an antibody against nucleolin (green) as a marker for the nucleolus, which is the characteristic localization of NuSAP in the interphase nucleus (blue), shows that the these two proteins localize independently. Scale bars in A, B and C, 10 μm.

tubulin signal at the pole, revealing distinct co-localization of the two proteins. In order to compare the INMAP dots in the interphase nucleus with the well-defined localization of NuSAP to nucleoli [9], we used double-staining with antibodies against nucleolin. As shown in Fig. 4F, the INMAP dots and the nucleolin signal were unrelated. The INMAP staining pattern was also unrelated to the pattern obtained with a monoclonal antibody against POLR3B (details not shown), further supporting the specificity of the anti-INMAP antibody. Thus, despite some similarities in the localization of INMAP relative to that of NuMA and NuSAP, clearly the INMAP is a distinct protein with unique localization pattern during the cell cycle.

Deletion analysis shows that the specific nuclear localization of INMAP is conferred by its C-terminus

Preliminary sequence analysis indicated that the specific subcellular localization of INMAP involves its C-terminus. Using PCR and oligonucleotide primers and *INMAP* cDNA as a template, we

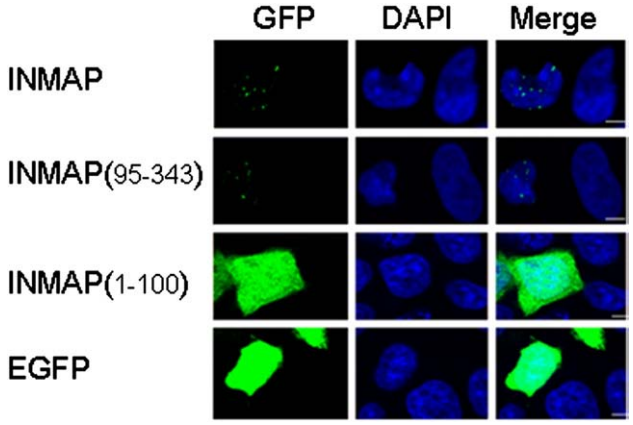

Fig. 5 – Deletion analysis using the expression of N- or C-terminal fragments of EGFP-INMAP in HeLa cells. HeLa cells were transiently transfected with pEGFP-C3 recombinant vectors encoding either intact INMAP or its N-terminal (aa 1–100) or C-terminal (aa 95–343) deletion fragments, and maintained in culture for two days. Confocal microscopy revealed that only cells expressing either the intact INMAP or its C-terminal fragment typically localized as distinct dots in the interphase nucleus, whereas cells expressing the N-terminal fragment showed a diffuse matrix of fine puncta throughout the cytoplasm and the nucleus, similar to the control EGFP. Scale bar, 10 μm.

prepared two deletion fragments corresponding to the N- and C-terminus of INMAP. The fragments were ligated into the expression vector pEGFP-C3 and the recombinant vector transiently transfected into HeLa cells. Confocal microscopy of cells expressing the GFP fusion protein showed that only the cells expressing either intact INMAP or its (aa 95–343) fragment exhibited the typical dots in the interphase nucleus (Fig. 5). By contrast, cells expressing the fragment (aa 1–100) gave only a diffuse GFP signal throughout the cytoplasm as well as nucleus similar to the control EGFP. Therefore the specific localization of INMAP to the nucleus is conferred by its C-terminal domain.

Co-immunoprecipitation of INMAP with α-tubulin, NuMA, and γ-tubulin

To examine whether the co-localization of INMAP with α-tubulin, NuMA and γ-tubulin in the mitotic spindle and cytokinetic midbody reflects their association in the same protein complex, we performed co-immunoprecipitation using antibodies against these proteins and total protein extracts from HeLa cells synchronized in M phase using nocodazole. Flow cytometry confirmed that almost all cells were at the G2/M phase (Fig. 6A). Analysis of the immunocomplexes by SDS-PAGE and Western immunoblotting using anti-INMAP, anti-NuMA, anti-γ-tubulin and anti-α-tubulin antibodies revealed that all four proteins do indeed co-immunoprecipitate, irrespective of whether the bait protein is INMAP, α-tubulin, NuMA, or γ-tubulin (Fig. 6B). None of the proteins appeared in the precipitate when using a monoclonal antibody against Golgin-245, which is known to localize specifically to Golgi [38], confirming the specificity of the co-immunoprecipitations. These results are consistent with the subcellular localization pattern obtained with the double immunolabeling using these antibodies in the above experiments.

Stable overexpression of INMAP impairs spindle formation, produces polycentrosomal and bi-nucleate cells, and inhibits cell growth and proliferation

To examine the functional role of INMAP, we overexpressed the protein by inserting a sense *INMAP* coding sequence into pcDNA3.1 (+) expression vector and transfecting it into HeLa cells. Cell lines stably expressing sense-*INMAP* or an empty vector were established using geneticin G418 selection [39] followed by two months of culturing. For analysis, the cells were sub-cultured for 2–3 days. Overexpression was assessed by staining protein gels with Coomassie blue (Fig. 7A) and by Western blotting using anti-INMAP monoclonal antibody (Fig. 7B). Both techniques showed that INMAP was effectively overexpressed. Densitometry of the Western blots using ImageQuant TL V2003.0.3 software [40] showed that both the 40-kDa and the 80-kDa bands were overexpressed by a factor of 1.9.

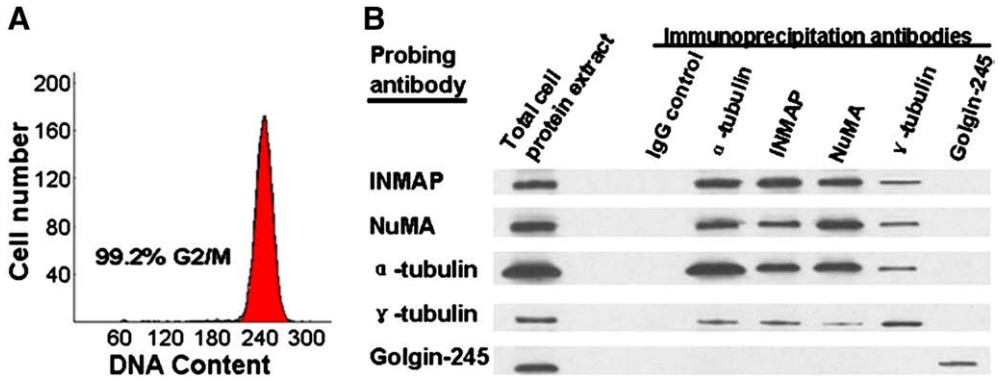

Fig. 6 – Co-immunoprecipitation of INMAP with NuMA, α-tubulin, and γ-tubulin. Total protein extracts were prepared from HeLa cells synchronized in M phase using nocodazole, incubated with specified antibodies, the resulting protein complexes were then precipitated, transferred to nitrocellulose membrane, and probed with individual antibodies. (A) Flow cytometry analysis showing that most cells were synchronized in the G2/M phase. (B) Immunoblots of protein complexes obtained by immunoprecipitation with antibodies against either α-tubulin, INMAP, NuMA, or γ-tubulin, and subsequently probed with individual antibodies (indicated on left). Invariably, all four proteins were detected in each of the immunoprecipitates, indicating the four proteins interact as a complex. Immunoprecipitations with an IgG control and anti-Golgin-245 were negative.

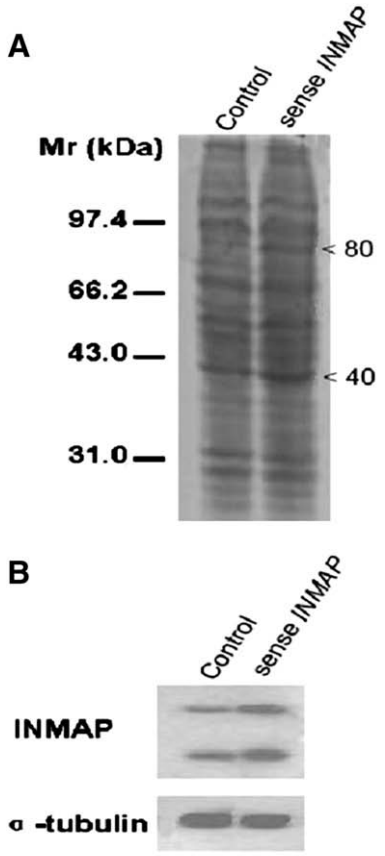

Control/Sense *INMAP*	The ratio of quantity
INMAP of 40 kDa	1.0 / 1.9
INMAP of 80 kDa	1.0 / 1.9
α-tubulin	1.0 / 1.0

Fig. 7 – Overexpression of INMAP in HeLa cell line stably transfected with sense-*INMAP*. HeLa cells were stably transfected with sense-*INMAP* or with control plasmid (pcDNA3.1 (+) no insert) the total cell proteins separated by SDS-PAGE, transferred onto nitrocellulose membrane and probed with antibodies. (A) Coomassie blue staining of protein gel. Arrows indicate polypeptide bands with Mr ~40 and ~80 kDa that were enriched in the sense-*INMAP* cells compared with the control. (B) Western blot analysis using a monoclonal antibody against INMAP and α-tubulin-antibody to check for equal protein loading. Immunoreaction with the anti-INMAP antibody again indicates greater amount of protein in the sense-*INMAP* cells for both the Mr ~40 and ~80-kDa bands compared with the control bands.

Overexpression of INMAP led to dramatic changes in cell morphology (Fig. 8A). The surface of some cells became wrinkled (thin arrow) and some cells appeared to split into smaller vesicles (thick arrow). Many rounded cells, resembling cells undergoing mitosis, appeared suspended in the medium. Flow cytometry analysis showed that cells typically accumulated at G2/M phase, with corresponding reduction in the proportion of cells at S phase (Fig. 8B). The analysis also revealed a small peak of cells with DNA content below the 2n level, which together with the morphological aberrations indicates that some cells became apoptotic. MTT growth curves showed that cell growth and proliferation was strongly inhibited, so that by day 4 in culture the growth of cells was reduced by about 50% and even more with continuous culturing (Fig. 8C). Thus, overexpression of INMAP apparently leads to aberrant cell morphology, inhibition of cell growth, and apoptosis.

To explore possible mechanisms of the reduced cell proliferation, we examined the cells microscopically using immunofluorescent staining of the centrosome with antibodies against γ-tubulin or centrin as centrosomal markers, and by DAPI staining of the nucleus. Many cells displayed multiple centrosomes (Figs. 9A, C). The proportions of cells with multiple centrosomes as revealed by the two antibodies were, respectively, 33.2 ± 1.5% and 33.0 ± 3.2.% in cells overexpressing INMAP, compared with 9.3 ± 1.5% and 8.1 ± 3.2. % in the controls (Figs. 9B, D). As shown by DAPI and α-tubulin staining, many cells overexpressing INMAP were binuclate or multinucleate or had fragmented nuclei (Fig. 9E). The proportion of bi- or multinucleate cells was 16.8 ± 1.5% in cells overexpressing INMAP, compared with 7.2 ± 1.2% in the controls (Fig. 9F).

In order to explore how overexpression of INMAP might affect the organization of the mitotic spindle, we released mitotic cells by gently shaking the culture plates, collected the free cells and processed them for immunofluorescence microscopy using labeling with anti-α-tubulin or anti γ-tubulin antibodies and counter-staining with DAPI. Flow cytometry analysis confirmed that most of these cells were in the G2/M phase (Fig. 10A). Microscopic examination revealed that, unlike the symmetrical bipolar spindle in the controls, in many cells overexpressing INMAP the structure of the mitotic spindle was dramatically distorted (Figs. 10B, D). Usually the spindle was multipolar, with prominent aster-like structures but lacking central spindle microtubules; in cells double-labeled with anti-γ-tubulin antibody, the focal point of the aster-like structures typically colocalized with γ-tubulin and presumably the centrosome (Fig. 10D). In some cells, only thick microtubule bundles of variable length formed the central spindle but without distinct asters at the poles.

It seems unlikely that cells with such dramatically distorted spindles would be able to accomplish segregation of chromatids at anaphase or complete cytokinesis. Quantitative assessment of the frequency of the aberrant spindles showed that the proportion of cells with aster-like structures was 34 ± 1.7% in cells overexpressing INMAP, compared with 4.7 ± 0.6% in the controls (Fig. 10C). Similarly, the proportion of cells with bundled spindle microtubules was 16 ± 1.0%, compared with 1.8 ± 1.2% in the controls. It is likely that the proportion of cells with multipolar spindles corresponds to the proportion of cells with multiple centrosomes (Figs. 9B, D) whereas the 16% cells with bundled spindle microtubules presumably have only two centrosomes (bottom panel in Fig. 10D).

Transient overexpression of INMAP produces aberrant phenotypes similar to those obtained with stable overexpression

In order to confirm that the phenotypes produced by stable INMAP overexpression in Figs. 8–10 were not due to non-specific responses caused by long term over-expression of INMAP, we performed transient transfection. HeLa cells were transfected with the pcDNA3.1 (+) expression vector with or without the sense-*INMAP* insert using Lipofectamine 2000 (Invitrogen, USA), and cultured for 36 h before processing for Western blotting, flow cytometry,

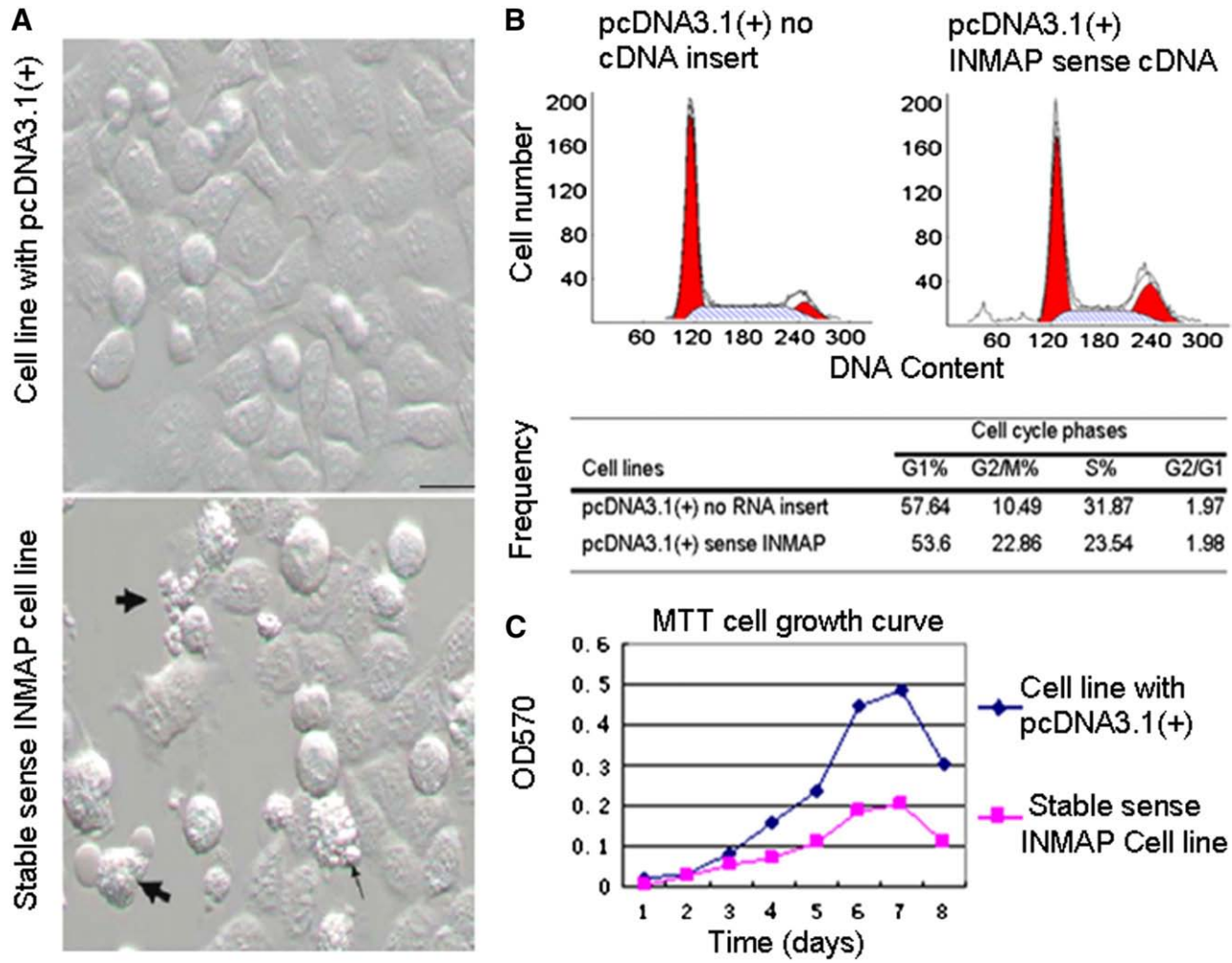

Fig. 8 – Disruption of cell morphology, growth and cycle progression in stable sense-*INMAP* HeLa cell line. (A) Aberrant morphology of cells overexpressing INMAP (arrows); Scale bars, 10 μm. (B) Flow cytometry analysis, showing that cell cycle was prominently stalled at G2/M phase along with reduction in S phase. (C) Cell growth curves determined by the MTT method, showing strong inhibition of cell growth.

and microscopic analysis as above. Western immunoblotting showed that the INMAP was strongly overexpressed (Fig. 11A). As before, the cell morphology was dramatically changed (Fig. 11B). The cells accumulated at G2/M phase and the DNA content was below the 2n level in some cells (Fig. 11C), and cell growth and proliferation was inhibited (Fig. 11D).

Staining with antibodies against γ-tubulin or centrin and confocal microscopy showed that the transient INMAP overexpression dramatically increased the frequency of centrosomal labeling about 8–10 fold relative to controls (Figs. 12A–D), compared with ~3 fold increase seen in the stable expression above. Double labeling cells synchronized in the G2/M phase with antibodies against α-tubulin and γ-tubulin again showed spindle abnormalities such as aster-like structures or bundled spindle microtubules as before (Figs. 13A–C). The transient INMAP overexpression increased the frequency of these abnormalities about 10-fold relative to controls, compared with ~7 fold increase seen in the stable expression above. Thus the brief, transient overexpression of INMAP is at least as effective, if not more, as the long-term stable transfection in producing the aberrant phenotypes.

Discussion

The assembly of bipolar mitotic spindle is known to involve the participation of numerous proteins, although a better understanding of the mechanism requires the identification of additional proteins. Recently we discovered a novel centrosome-related protein Crp^{F46} of Mr ~60 kDa by using autoantiserum F46 from a patient with progressive systemic sclerosis to immunoprecipitate target proteins from HeLa cell extracts [27]. In the present study we have identified the gene for an additional novel protein by screening HeLa cDNA expression library with the autoantiserum F46. This new gene showed high similarity to the 3′-end of an unnamed, uncharacterized gene (GenBank accession no. 7022388). Because this gene lacked a definitive translation initiation site, we used 5′-RACE and bioinformatics to obtain full-length cDNA. MS/MS sequencing of a polypeptide band obtained by immunoprecipitation from HeLa cells using the autoantiserum F46 showed that the amino-acid sequence is identical to the predicted protein sequence of the unnamed gene, with a predicted molecular mass of 38.2 kDa. According to characterization

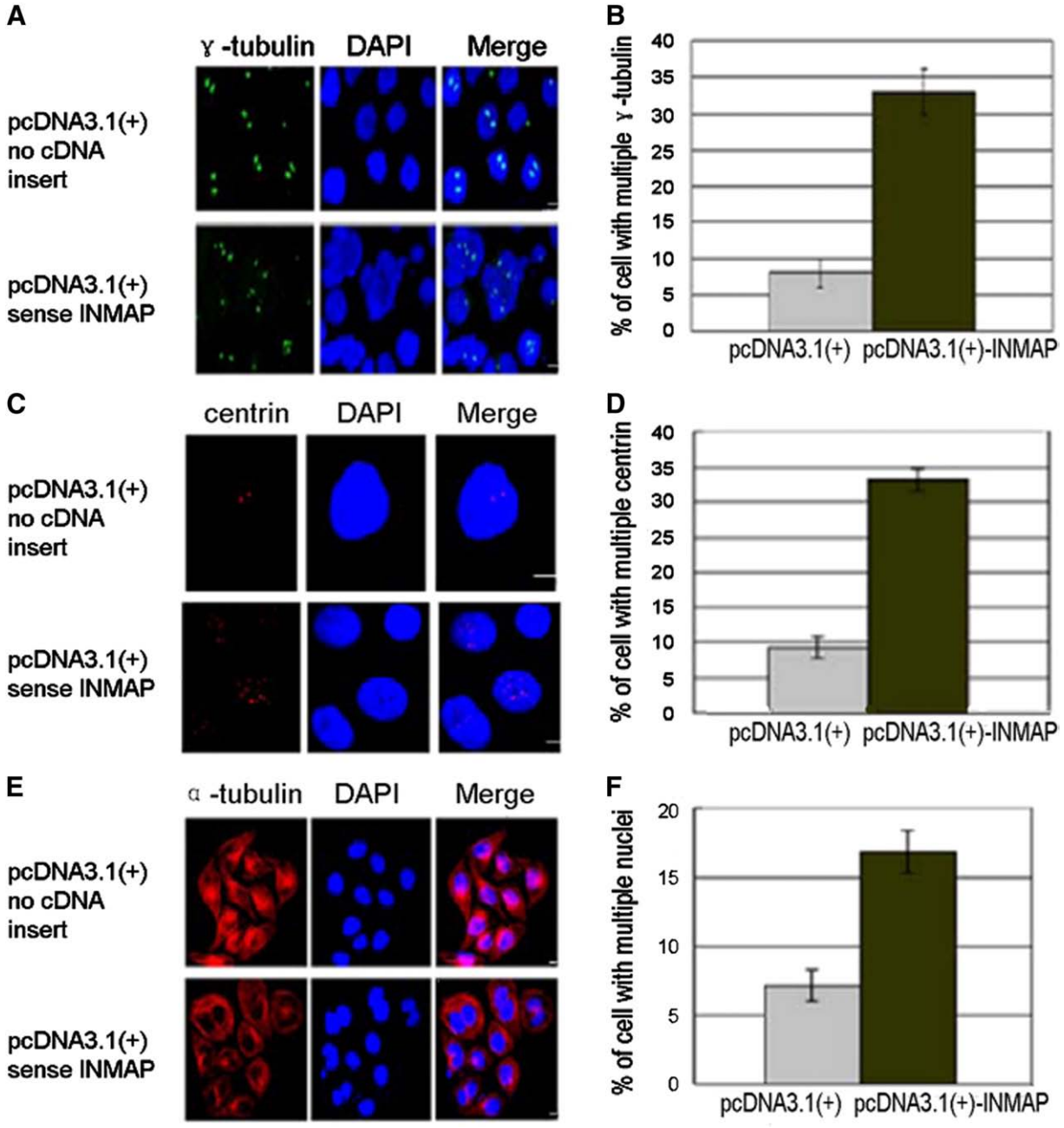

Fig. 9 – Mitotic defects in stable sense-*INMAP* HeLa cell line. Sense-*INMAP* or control HeLa cells were immunolabeled using anti-γ-tubulin, anti-centrin, or anti-α-tubulin polyclonal antibodies, counter-stained with DAPI to label DNA, and examined in a confocal microscope. (A) Immunofluorescence images of control cells and sense-*INMAP* cells labeled with anti-γ-tubulin antibody (green), showing multiple centrosomes in large nuclei in cells overexpressing INMAP. (B) Quantitative analysis of the proportions of cells with multiple centrosomes. (C) Immunofluorescence images of cells labeled with anti-centrin antibody (red). (D) Quantitative analysis of the proportion of cells with multiple centrosomes. (E) Immunofluorescence images of cells labeled with anti-α-tubulin antibody, showing bi-nucleate cells and nuclear fragments in cells overexpressing INMAP. (F) Quantitative analysis of the proportions of cells with multiple nuclei in cells overexpressing INMAP. Data in B, D, and F are the means and SD of 200 cells in each of three independent experiments. Scale bars in A, C, and E, 10 μm.

by microscopic analysis of cells during the cell cycle, deletion analysis, and co-immunoprecipitation with spindle-marker proteins, we named the protein Interphase Nucleus and Mitotic apparatus Associated Protein (INMAP). Immunoblotting using a monoclonal antibody against INMAP cross-reacted with similar polypeptides in Mel cells and *S. cerevisiae*. BLAST search of NCBI protein database revealed that the protein is highly conserved through evolution, indicating that INMAP plays an important role in eukaryotes.

Microscopic analysis using either GFP-INMAP fusion protein in living cells or immunofluorescence labeling using a monoclonal

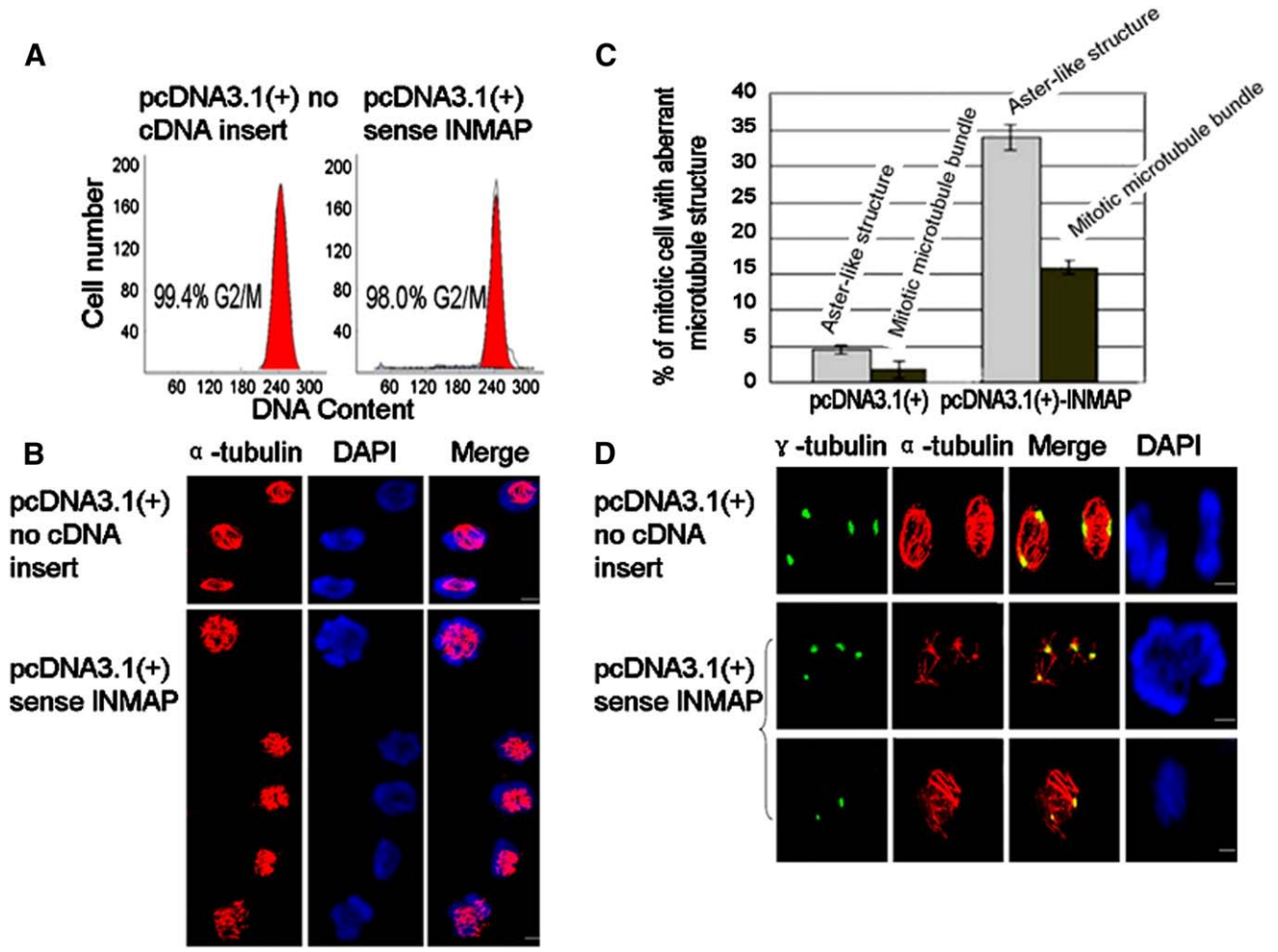

Fig. 10 – Aberrant mitotic spindles in stable sense-*INMAP* mitotic HeLa cell line. Mitotic cells were obtained by gently shaking the culture plates to release the cells and collecting them; the cells were then labeled for immunofluorescence microscopy using antibodies against α-tubulin or γ-tubulin or both, counter-stained with DAPI, and examined in a confocal microscope. (A) Flow cytometry analysis showing that most cells were in the G2/M phase. (B) Immunofluorescence labeling of α-tubulin in cells overexpression INMAP shows dramatic distortions in the structural organization of the mitotic spindle, mostly as multipolar spindles with prominent aster-like structures or alternatively thick microtubule bundles of the central spindle without distinct polar asters (see also D). (C) Quantitative assessment of the frequency of cells with aberrant spindles. Data are the means and SD of 200 cells in each of three independent experiments. (D) Double immunofluorescence labeling using polyclonal antibodies against γ-tubulin (green) and α-tubulin (red). The focal points of aster-like structures clearly co-localize (yellow in Merge) with centrosomal γ-tubulin, whereas the thick microtubule bundles of the central spindle seem to be only loosely connected to the centrosome. Scale bars in B and D, 10 μm.

antibody against INMAP in fixed cells both showed that INMAP consistently localized to the nucleus during interphase and re-localized to the spindle at the onset of mitosis. Localization to the interphase nucleus appeared as distinct dots, about 10–15 per nucleus, and was conferred by amino acid residues 95–343 in the C-terminal portion of INMAP as revealed by deletion analysis. During mitosis/M phase, INMAP associated with all components of the spindle including the poles and microtubules of the central spindle, and with the midbody during telophase/cytokinesis. In addition, double-immunostaining using specific antibodies showed that INMAP co-localized closely with the spindle-marker proteins α-tubulin and NuMA, and with the centrosomal marker proteins γ-tubulin. Significantly, all these proteins also co-purified in their native state as a complex during co-immunoprecipitation using individual antibodies against these proteins, irrespective of which antibody-protein bait was used. Clearly, INMAP localizes in a cell cycle-dependent manner, suggesting that it is closely related to the process of mitotic spindle assembly.

It is likely that the cell cycle-dependent redistribution of INMAP involves phosphorylation through its 14 predicted phosphorylation sites, including a main phosphorylation site for cdc2. The localization and function of numerous proteins generally depends on their modifications including phosphorylation. The mitotic kinesin Eg5 is a typical case in which mutation of the phosphorylation site threonine (T937) abolishes its association with the spindle [41]. The redistribution of INMAP from the interphase

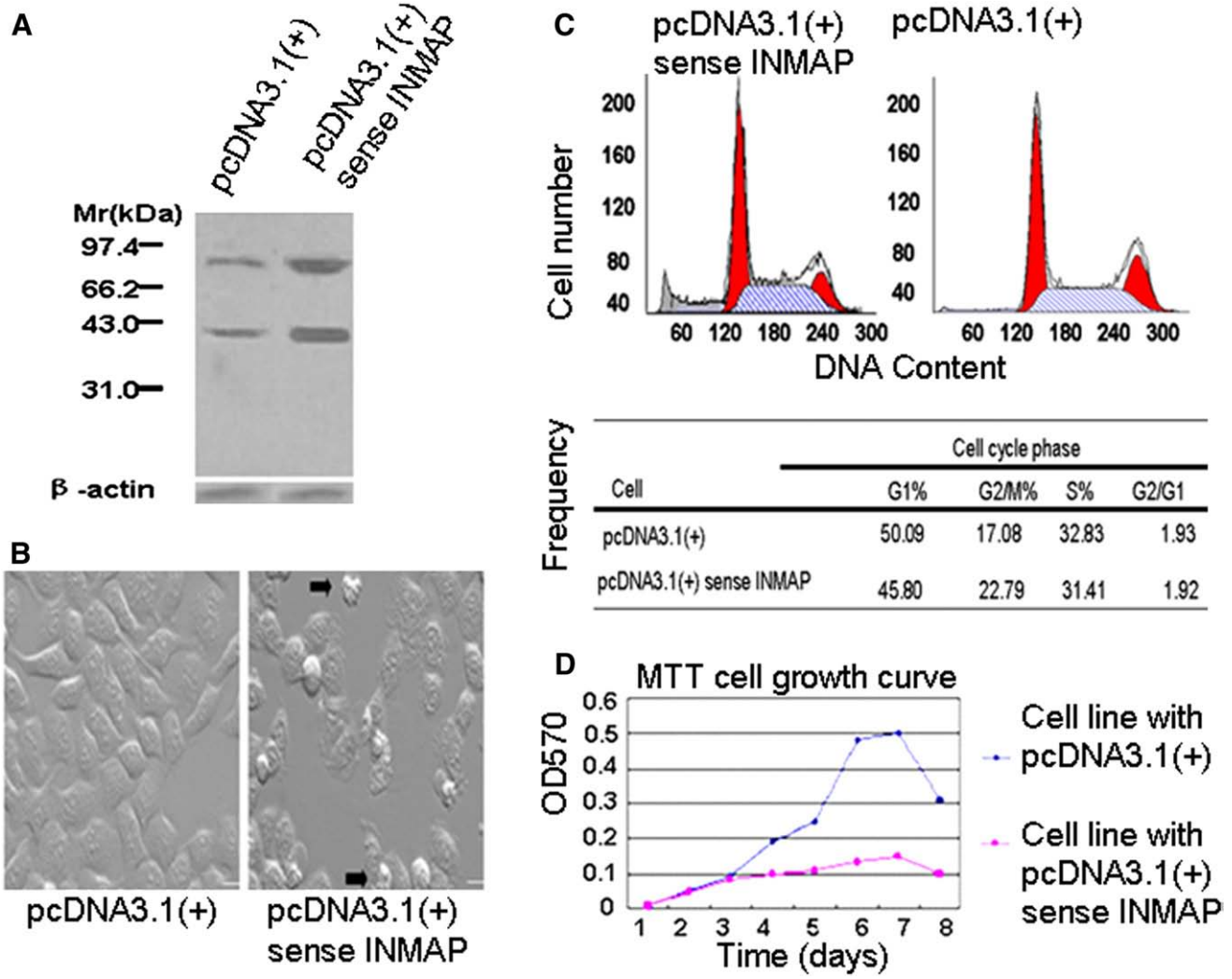

Fig. 11 – Disruption of cell morphology, growth and cycle progression in HeLa cells after 36 h of transient transfection with sense-*INMAP*. (A) Western blot showing distinct overexpression of INMAP. (B) Cells with aberrant morphology (arrows); Scale bars, 10 μm. (C) Flow cytometry analysis, showing that cell cycle was stalled at G2/M phase. (D) Cell growth curves determined by the MTT method, showing strong inhibition of cell growth.

nucleus to the mitotic apparatus may also involve phosphorylation along with nuclear envelope breakdown. Interestingly, treatment of HeLa proteins with 8 M urea followed by immunoblotting with the anti-INMAP antibody showed that the ~80-kDa polypeptide is a dimer of 40 kDa, close to the predicted molecular mass of INMAP of 38.2 kDa. Furthermore, our preliminary experiments with synchronized HeLa cells have revealed that only the 40-kDa monomer is present in interphase cells whereas mitotic cells possess both the 40-kDa and the 80-kDa forms (data not shown). Thus the potential phosphorylation status of INMAP, its apparent dimerization, and subcellular relocalization are all likely to be cell-cycle related. A detailed investigation is in progress.

The cell cycle-dependent localization of INMAP to the spindle is of eminent interest since the mitotic apparatus is crucial for the process of cell division. Formation of the spindle involves dramatic changes in microtubule rearrangement and the recruitment of specific spindle-associated proteins in order to function properly in the mitotic phase [12,43–47]. Proteins such as NuMA and NuSAP have been shown to localize to the nucleus during interphase and to undergo cell cycle-dependent re-localization specifically to the spindle during the mitosis. These proteins are essential for maintaining the integrity of the spindle as documented by manipulating the expression levels in knockdown or overexpression experiments, which disrupt the formation of the spindle and inhibit cell cycle progression [9,21,48,49]. These features are very similar to the novel protein INMAP. Overexpression of INMAP likewise caused dramatic changes in cellular morphology, disrupted the formation of the mitotic spindle, induced apoptosis, and inhibited cell cycle progression and cell proliferation. INMAP is distinct from the nucleolar localization of NuSAP since its localization in the interphase nucleus is spatially separated from localization of nucleolin. Thus, as in many conserved proteins that have been identified to perform vital function on the growth and proliferation of cells, including ICF45, Rheb GTPase, Caprin-1, Drf1/ASKL1 and THAP1 [26,50–53], INMAP likewise plays a critical role.

One striking effect of overexpressing INMAP was the formation of polycentrosomal and binucleate cells. Many proteins are known to influence the centrosome and mitosis. For example, altered

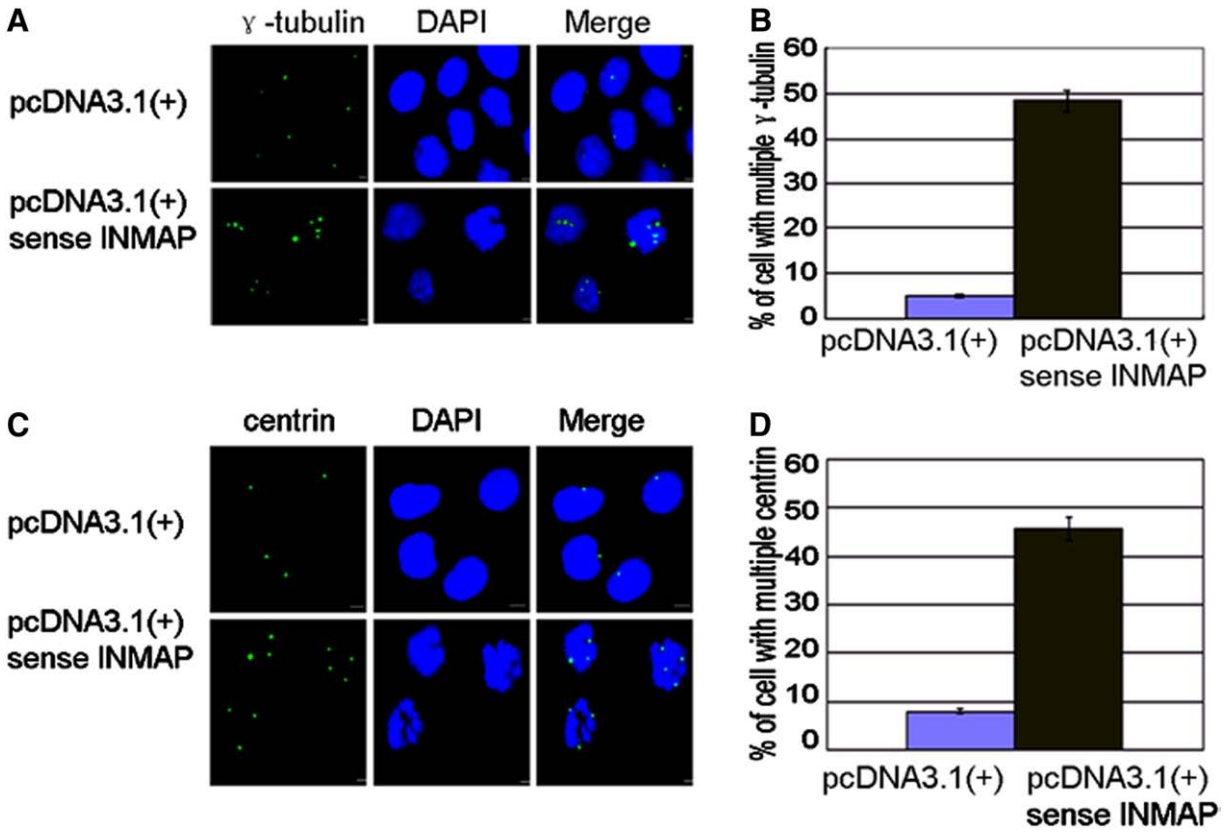

Fig. 12 – Multiple centrosomal labeling in HeLa cells after 36 h of transient transfection with sense-*INMAP*. Cells were immunolabeled using anti-γ-tubulin or anti-centrin antibodies, counter-stained with DAPI, and examined in a confocal microscope. (A, C) Immunofluorescence images of cells labeled with anti-γ-tubulin or anti-centrin antibody (green), showing multiple centrosomal labeling in cells overexpressing INMAP; Scale bars in A and C, 10 μm. (B, D) Frequency of cells with multiple γ-tubulin or centrin centrosomal labeling. Data in B, D are the means and SD of 200 cells in each of three independent experiments.

expression of centrosome-related proteins like Stat3, Pin1 and CDC25B resulted in centrosome overduplication and formation of multinucleate cells [4,54–57], and similar aberrations resulted from altered expression of the spindle-related proteins NuSAP and TMAP/CKAP2 [9,58]. However, it appears there are at least two alternative mechanisms by which these proteins can act on the centrosome and mitosis. Abnormal expression of some proteins, such as Pin1 and CDC25B, may directly result in centrosomal overduplication followed by the formation of multinucleate cells [4,57], whereas other proteins, such as NuSAP, may cause failure of cytokinesis and consequently the appearance of multiple centrosomes in multinucleate cells [9]. In the case of INMAP the more likely explanation is failure of cytokinesis, although we have not eliminated centrosomal overduplication because overexpressing INMAP might also alter the expression of centrosomal regulatory proteins.

Another striking effect of INMAP overexpression was the formation of aberrant mitotic spindles and consequently failure of mitosis and inhibition of cell cycle progression. Many spindle-associated proteins have been shown to play vital roles in the formation of bipolar spindle or maintaining its integrity, for example, NuSAP, TMAP/CKAP2, Nup107–160, Dynein/dynactin, Rae1 and NuMA [5,9,21,42,58–63]. Additionally, aberrations in spindle structure caused by deletion or overexpression of one protein can be counteracted by similar deletion or overexpression of another protein, thereby rescuing spindle bipolarity and showing that the levels of these proteins must be balanced. For example, the deleterious effects of depletion or overexpression of NuMA were counteracted by proportional depletion or overexpression of Rae1 [42]. In the case of INMAP, overexpression dramatically disrupted the formation of the mitotic spindle in about 50% of the total mitotic cells, leading to the formation of prominent, multiple aster-like structures or alternatively thick microtubule bundles in the central spindle without distinct polar asters. These abnormalities are similar to those resulting from overexpressing NuSAP or TMAP/CKAP2, which lead to the formation of aberrant microtubule bundles in the central spindle [9] or abnormal aster-like structures [58]. Moreover, double inmmunostaining assay of INMAP with antibodies against α-tubulin or γ-tubulin confirmed that the aster-like structures associate closely with the centrosome, whereas the thick microtubule bundles in the central spindle appeared to be only loosely connected to the centrosome, indicating that INMAP overexpression affected the normal association of microtubules with the centrosome. Possibly an excessive cross-linking of microtubules into thick bundles over-rides the normal microtubule-organizing function of the centrosome. Departure from normal bipolar spindle into the two opposite extremes – either prominent polar aster-like structures or thick microtubule bundles in the central spindle – may reflect the degree of overexpression in

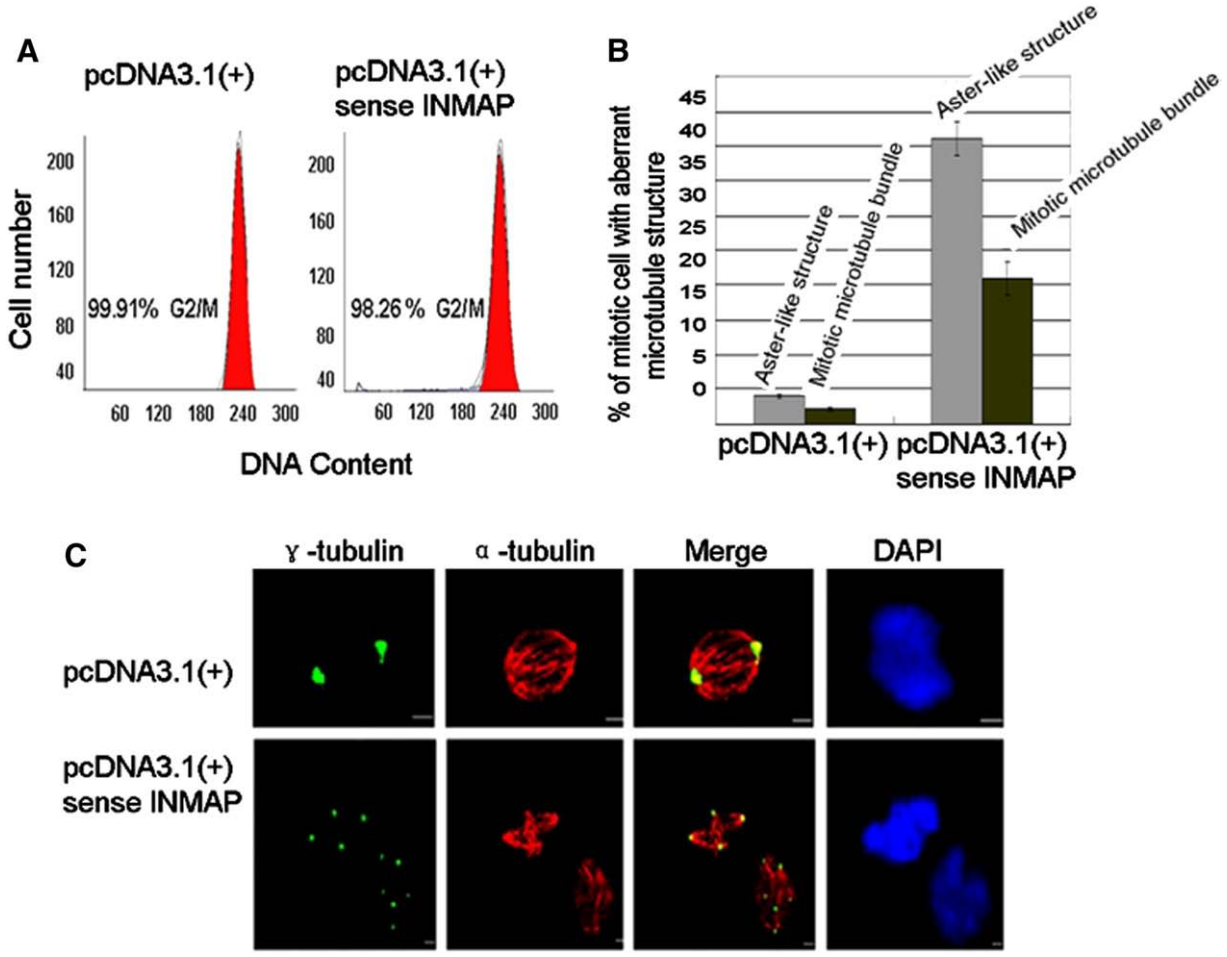

Fig. 13 – Aberrant mitotic spindles in HeLa cells after 36 h of transient transfection with sense-*INMAP*. Mitotic cells were labeled for immunofluorescence microscopy using antibodies against α-tubulin and γ-tubulin, counter-stained with DAPI, and examined in a confocal microscope. (A) Flow cytometry analysis showing that most cells were in the G2/M phase. (B) Frequency of cells with aberrant mitotic spindles. Data are the means and SD of 200 cells in each of three independent experiments. (C) Double immunofluorescence labeling using polyclonal antibodies against γ-tubulin (green) and α-tubulin (red). Scale bars, 10 μm.

individual cells. In either extreme the spindle is apparently dysfunctional, leading to production of binucleate or multinucleate cells or nuclear fragments, and consequently to disruption in the progression of the normal cell cycle and cell proliferation.

In conclusion, our study has identified a novel interphase nucleus- and mitotic spindle-associated protein, INMAP, a conserved protein with cell cycle-dependent localization and essential role in the formation of normal, bipolar mitotic spindle and cell cycle-progression. Experiments are in progress to further elucidate the function of this protein including the mechanism of its phosphorylation, dimerization and role in centrosome duplication, mitosis, and cytokinesis.

Acknowledgments

We thank Drs. Yongzhe Li and Jingtao Cui (Peking Union Medical College, Chinese Academy of Medical Science, China) for providing autoimmune-sera, M.S Zhitao Rong (Beijing Normal University, China) for a gift of pcDNA3.1 (+)-neo Vector, and Dr. Yue Wang (Institute of Molecular and Cell Biology, A-STAR, Singapore) for help in protein sequencing. This work was supported by the National Natural Science Foundation of China grant nos. 30771101 and 30470875 to Q.L., a fund from the Key Laboratory of Cell Proliferation and Regulation Biology of Ministry of Education of China, and a fund from Beijing Normal University that supports the Key Lab for the Subject of Developmental Biology. We also thank two anonymous reviewers for their suggestions for improvement.

REFERENCES

[1] H.C. Joshi, M.J. Palacios, L. Mcnamara, D.W. Cleveland, γ-Tubulin is a centrosomal protein required for cell cycle-dependent microtubule nucleation, Nature 356 (1992) 80–83.
[2] N. Delgehyr, J. Sillibourne, M. Bornens, Microtubule nucleation and anchoring at the centrosome are independent processes linked by ninein function, J. Cell Sci. 118 (2005) 1565–1575.
[3] D.K. Moss, G. Bellett, J.M. Carter, M. Liovic, J. Keynton, A.R. Prescott, E.B. Lane, M.M. Mogensen, Ninein is released from the centrosome and moves bi-directionally along microtubules, J. Cell Sci. 120 (2007) 3064–3074.

[4] F. Suizu, A. Ryo, G. Wulf, J. Lim, K.P. Lu, Pin1 regulates centrosome duplication, and its overexpression induces centrosome amplification, chromosome instability, and oncogenesis, MCB (2006) 1463–1479.
[5] Q. Liu, J.V. Ruderman, Aurora A, mitotic entry, and spindle bipolarity, PNAS 103 (2006) 5811–5816.
[6] A. Merdes, R. Heald, K. Samejima, W.C. Earnshaw, D.W. Cleveland, Formation of spindle poles by dynein/dynactin-dependent transport of NuMA, J. Cell Biol. 149 (2000) 851–861.
[7] T. Wittmann, M. Wilm, E. Karsenti, I. Vernos, TPX2, a novel *Xenopus* MAP involved in spindle pole organization, J. Cell Biol. 149 (2000) 1405–1418.
[8] S.L. Rogers, G.C. Rogers, D.J. Sharp, R.D. Vale, *Drosophila* EB1 is important for proper assembly, dynamics, and positioning of the mitotic spindle, J. Cell Biol. 158 (2002) 873–884.
[9] T. Raemaekers, K. Ribbeck, J. Beaudouin, W. Annaert, M.V. Camp, I. Stockmans, N. Smets, R. Bouillon, J. Ellenberg, G. Carmeliet, NuSAP, a novel microtubule-associated protein involved in mitotic spindle organization, J. Cell Biol. 162 (2003) 1017–1029.
[10] S.C. Huang, R. Jagadeeswaran, E.S. Liu, E.J. Benz Jr., Protein 4.1R, a microtubule-associated protein involved in microtubule aster assembly in mammalian mitotic extract, J. Biol. Chem. 279 (2004) 34595–34602.
[11] J.M. Saffin, M. Venoux, C. Prigent, J. Espeut, F. Poulat, D. Giorgi, A. Abrieu, S. Rouquier, ASAP, a human microtubule-associated protein required for bipolar spindle assembly and cytokinesis, PNAS 102 (2005) 11302–11307.
[12] M. Kimura, S. Kotani, T. Hattori, N. Sumi, T. Yoshioka, K. Todokoro, Y. Okano, Cell cycle-dependent expression and spindle pole localization of a novel human protein kinase, Aik, related to Aurora of *Drosophila* and yeast Ip11, J. Biol. Chem. 272 (1997) 13766–13771.
[13] J.A. Kahana, D.W. Cleveland, Beyond nuclear transport: Ran-GTP as a determinant of spindle assembly, J. Cell Biol. 146 (1999) 1205–1209.
[14] M. Hetzer, O.J. Gruss, I.W. Mattaj, The Ran GTPase as a marker of chromosome position in spindle formation and nuclear envelope assembly, Nat. Cell Biol. 4 (2002) E177–E184.
[15] A.J. Faragher, A.M. Fry, Nek2A kinase stimulates centrosome disjunction and is required for formation of bipolar mitotic spindles, Mol. Biol. Cell 14 (2003) 2876–2889.
[16] J. Luders, T. Stearns, Microtubule-organizing centres: a re-evaluation, Nat. Rev. Mol. Cell Biol. 8 (2007) 161–167.
[17] Q. Liu, J.V. Ruderman, Aurora A, mitotic entry, and spindle bipolarity, Proc. Natl. Acad. Sci. U. S. A. 103 (2006) 5811–5816.
[18] A.R. Barr, F. Gergely, Aurora-A: the maker and breaker of spindle poles, J. Cell Sci. 120 (2007) 2987–2996.
[19] C.H. Yang, E.J. Lambie, M. Snyder, NuMA: an unusually long coiled-coil related protein in the mammalian nucleus, J. Cell Biol. 116 (1992) 1303–1317.
[20] N.J. Quintyne, J.E. Reing, D.R. Hoffelder, S.M. Gollin, W.S. Saunders, Spindle multipolarity is prevented by centrosomal clustering, Science 307 (2005) 127–129.
[21] K. Ribbeck, A.C. Groen, R. Santarella, M.T. Bohnsack, T. Raemaekers, T. Köcher, M. Gentzel, D. Görlich, M. Wilm, G. Carmeliet, T.J. Mitchison, J. Ellenberg, A. Hoenger, I.W. Mattaj, NuSAP, a mitotic RanGTP target that stabilizes and cross-links microtubules, Mol. Biol. Cell 17 (2006) 2646–2660.
[22] Y. Moroi, C. Peebles, M.J. Fritzler, J. Steigerwald, E.M. Tan, Autoantibody to centromere (kinetochore) in scleroderma sera, Proc. Natl. Acad. Sci. U. S. A. 77 (1980) 1627–1631.
[23] E.M. Tan, Antinuclear antibodies: diagnostic markers for autoimmune diseases and probes for cell biology, Adv. Immunol. 44 (1989) 93–151.
[24] H.J. Ditzel, Human antibodies in cancer and autoimmune disease, Immunol. Res. 21 (2000) 185–193.
[25] C.H. Yang, E.J. Lambie, M. Snyder, NuMA: an unusually long coiled-coil related protein in the mammalian nucleus, J. Cell Biol. 116 (1992) 1303–1317.
[26] D.L. Guo, K. Hu, Y. Lei, Y.C. Wang, T.L. Ma, D.C. He, Identification and characterization of a novel cytoplasm protein ICF45 that is involved in cell cycle regulation, J. Biol. Chem. 279 (2004) 53498–53505.
[27] Y. Wei, E.Z. Shen, N. Zhao, Q. Liu, J.L. Fan, J. Marc, Y.C. Wang, L. Sun, Q.J. Liang, Identification of a novel centrosomal protein CrpF46 involved in cell cycle progression and mitosis, Exp. Cell Res. 314 (2008) 1693–1707.
[28] R.S. Johnson, J.A. Taylor, Sequence database searches via *de novo* peptide sequencing by tandem mass spectrometry, Mol. Biotechnol. 22 (2002) 301–315.
[29] V. Dancik, T.A. Addona, K.R. Clauser, J.E. Vath, P.A. Pevzner, De novo peptide sequencing via tandem mass spectrometry: a graph-theoretical approach, J. Comput. Biol. 6 (1999) 327–342.
[30] T. Chen, M.Y. Kao, M. Tepel, J. Rush, G.M. Church, A dynamic programming approach for *de novo* peptide sequencing via tandem mass spectrometry, J. Comput. Biol. 8 (2001) 325–337.
[31] B. Lu, T. Chen, A suboptimal algorithm for *de novo* peptide sequencing via tandem mass spectrometry, J. Comput. Biol. 10 (2003) 1–12.
[32] N.S. Yee, W.L. Gong, Y. Huang, K. Lorent, A.C. Dolan, R.J. Mararia, M. Pack, Mutation of RNA Pol III subunit rpc2/polr3b leads to deficiency of subunit Rpc11 and disrupts zebrafish digestive development, PloS Biol. 5 (2007) 2484–2492.
[33] M.D. Sheets, S.C. Ogg, M.P. Wickens, Point mutations in AAUAAA and the poly (A) addition site: effects on the accuracy and efficiency of cleavage and polyadenylation in vitro, Nucleic Acids Res. 18 (1990) 5799–5805.
[34] M.R. Wilkins, I. Lindskog, E. Gasteiger, A. Bairoch, J.C. Sanchez, D.F. Hochstrasser, R.D. Appel, Detailed peptide characterization using PEPTIDEMASS—a World-Wide-Web-accessible tool, Electrophoresis 18 (1997) 403–408.
[35] N. Blom, S. Gammeltoft, S. Brunak, Sequence- and structure-based prediction of eukaryotic protein phosphorylation sites, J. Mol. Biol. 294 (1999) 1351–1362.
[36] N. Blom, T. Sicheritz-Ponten, R. Gupta, S. Gammeltoft, S. Brunak, Prediction of post-translational glycosylation and phosphorylation of proteins from the amino acid sequence, Proteomics 4 (2004) 1633–1649.
[37] F.S. Altschul, J.C. Wootton, E.M. Gertz, R. Agarwala, A. Morgulis, A.A. Schäffer, Y.K. Yu, Protein database searches using compositionally adjusted substitution matrices, J. FEBS 272 (2005) 5101–5109.
[38] J. Kooy, B. Toh-H, J.M. Pettitt, R. Erlich, P.A. Gleeson, Human autoantibodies as reagents to conserved Golgi components, J. Biol. Chem. 267 (1992) 20255–20263.
[39] E.U. Saelman, P.J. Keely, S.A. Santoro, Loss of MDCK cell alpha 2 beta 1 integrin expression results in reduced cyst formation, failure of hepatocyte growth factor/scatter factor-induced branching morphogenesis, and increased apoptosis, J. Cell Sci. 108 (1995) 3531–3540.
[40] W. Yang, J.J. Li, S. Hekimi, A measurable increase in oxidative damage due to reduction in superoxide detoxification fails to shorten the life span of long-lived mitochondria of *Caenorhabditis elegans*, Genetics 177 (2007) 2063–2074.
[41] K.E. Sawin, T.J. Mitchison, Mutations in the kinesin-like protein Eg5 disrupting localization to the mitotic spindle, Proc. Natl. Acad. Sci. U. S. A. 92 (1995) 4289–4293.
[42] R.W. Wong, G. Blobel, E. Coutavas, Rae1 interaction with NuMA is required for bipolar spindle formation, PNAS 103 (2006) 19783–19787.
[43] J.C. Waters, E. Salmon, Pathways of spindle assembly, Curr. Opin. Cell Biol. 9 (1997) 37–43.
[44] R. Heald, C.E. Walczak, Microtubule-based motor function in mitosis, Curr. Opin. Struc. Biol. 9 (1999) 268–274.
[45] T. Gaglio, A. Saredi, D.A. Compton, NuMA is required for the organization of microtubules into aster-like mitotic arrays, J. Cell Biol. 131 (1995) 693–708.

[46] A. Wilde, S.B. Lizarraga, L.J. Zhang, C. Wiese, N.R. Gliksman, C.E. Walczak, Y.X. Zheng, Ran stimulates spindle assembly by altering microtubule dynamics and the balance of motor activities, Nat. Cell Biol. 3 (2001) 221–227.
[47] L.C. Kapitein, E.J.G. Peterman, B.H. Kwok, J.H. Kim, T.M. Kapoor, C.F. Schmidt, The bipolar mitotic kinesin Eg5 moves on both microtubules that it crosslinks, Nature 435 (2005) 114–117.
[48] T.K. Tang, C.C. Tang, Y.J. Chao, C.W. Wu, Nuclear mitotic apparatus protein (NuMA): spindle association, nuclear targeting and differential subcellular localization of various NuMA isoforms, J. Cell Sci. 107 (1994) 1389–1402.
[49] N.J. Quintyne, J.E. Reing, D.R. Hoffelder, S.M. Gollin, W.S. Saunders, Spindle multipolarity is prevented by centrosomal clustering, Science 307 (2005) 127–129.
[50] P.H. Patel, N. Thapar, L. Guo, M. Martinez, J. Maris, C.L. Gau, J.A. Lengyel, F. Tamanoi, *Drosophila* Rheb GTPase is required for cell cycle progression and cell growth, J. Cell Sci. 116 (2003) 3601–3610.
[51] B. Wang, M.D. David, J.W. Schrader, Absence of Caprin-1 results in defects in cellular proliferation, J. Immunol. 175 (2005) 4274–4282.
[52] N. Yoshizawa-Sugata, A. Ishii, C. Taniyama, E. Matsui, K. Arai, H. Masai, A second human Dbf4/ASK-related protein, Drf1/ASKL1, is required for efficient progression of S and M phases, J. Biol. Chem. 280 (2005) 13062–13070.
[53] C. Cayrol, C. Lacroix, C. Mathe, V. Ecochard, M. Ceribelli, E. Loreau, V. Lazar, P. Dessen, R. Mantovani, L. Aguilar, J. Girard, The THAP-zinc finger protein THAP1 regulates endothelial cell proliferation through modulation of Prb/E2F cell-cycle target genes, Blood 109 (2007) 584–594.
[54] B. Metge, S. Ofori-Acquah, T. Stevens, R. Balczon, Stat3 activity is required for centrosome duplication in Chinese hamster ovary cells, J. Biol. Chem. 279 (2004) 41801–41806.
[55] T. Nishimura, M. Takahashi, H.S. Kim, H. Mukai, Y. Ono, Centrosome-targeting region of CG-NAP causes centrosome amplification by recruiting cyclin E-cdk2 complex, Genes Cells 10 (2005) 75–86.
[56] Z.Y. Ma, M. Kanai, K. Kawamura, K. Kaibuchi, K.Q. Ye, K. Fukasawa, Interaction between ROCK II and Nucleophosmin/B23 in the regulation of centrosome duplication, MCB 26 (2006) 9016–9034.
[57] R. Boutros, V. Lojois, B. Ducommun, CDC25B involvement in the centrosome duplication cycle and in microtubule nucleation, Cancer Res. 67 (2007) 11557–11564.
[58] K.U. Hong, Y.S. Park, Y.S. Seong, D.M. Kang, C.D. Bae, J. Park, Functional importance of the anaphase-promoting complex-Cdh1-mediated degradation of TMAP/CKAP2 in regulation of spindle function and cytokinesis, MCB 27 (2007) 3667–3681.
[59] N. Trieselmann, S. Armstrong, J. Rauw, A. Wilde, Ran modulates spindle assembly by regulating a subset of TPX2 and Kid activities including Aurora A activation, J. Cell Sci. 116 (2003) 4791–4798.
[60] O.J. Gruss, I. Vernos, The mechanism of spindle assembly: functions of Ran and its target TPX2, J. Cell Biol. 166 (2004) 949–955.
[61] A.V. Orjalo, A. Arnaoutov, Z.X. Shen, Y. Boyarchuk, S.G. Zeitlin, B. Fontoura, S. Briggs, M. Dasso, D.J. Forbes, The Nup107–160 nucleoporin complex is required for correct bipolar spindle assembly, Mol. Biol. Cell 17 (2006) 3806–3818.
[62] J. Gaetz, T.M. Kapoor, Dynein/dynactin regulate metaphase spindle length by targeting depolymerizing activities to spindle poles, J. Cell Biol. 166 (2004) 465–471.
[63] R.A. Green, R. Wollman, K.B. Kaplan, APC and EB1 function together in mitosis to regulate spindle dynamics and chromosome alignment, Mol. Biol. Cell 16 (2005) 4609–4622.